NEUTRON SCATTERING RESEARCH

at Rutherford Appleton Laboratory

Reprinted from "Rutherford Appleton Laboratory 1985"

Neutron Scattering Research

After years of planning and construction, ISIS, the RAL spallation neutron source, began operation in 1985. Following the successful production of neutrons at the first attempt in December 1984, regular running began in June. This continued until September, the intensity being increased to 10 μA of 550 MeV protons at the target. This was achieved at 25 pulses/second and 2.5×10^{12} protons/pulse (ppp), compared with the design performance of 50 pulses/second at 2.5×10^{13} ppp. During this period, commissioning of the six scheduled instruments and the three development instruments began and the first scientific experiments were performed. The neutron beam characteristics and instrument performances met design specifications and the first neutron scattering results are of high quality. Following the inauguration and naming ceremonies in October, work continued until December aimed at improving machine reliability and beam stability, minimising beam loss and increasing beam intensity.

In addition to the work on ISIS, the Laboratory continued to provide support for university and polytechnic research at Institut Laue-Langevin (ILL), Grenoble.

ISIS, the Spallation Neutron Source

On 1 October, ISIS was named by the Prime Minister and its research programme inaugurated. The Prime Minister was accompanied by the Secretary of State for Education and Science, the Rt Hon Sir Keith Joseph MP, Science Ministers from Italy, Luxembourg and Spain and representatives of Ministers from France, the Netherlands, Austria, Eire and West Germany. Altogether, about 140 government officials and scientists were present from the UK and abroad (Plate XII). Also present were Press, TV and Radio correspondents and Laboratory staff directly involved in the building of ISIS and its instruments. On the

following day, the facility was opened to visitors from Industry, universities and other scientific establishments. On 5 October, Laboratory staff and their families visited ISIS.

Accelerator and Target Station Commissioning

The run which produced first neutrons in December 1984 was at low current (about 1 pulse/second at 5×10^{11} ppp). Between January and June this year, much effort was devoted to achieving higher currents. The injector ion source and pre-injector were run at 25 Hz. Some unexpected effects were found on the pre-injector as described below. The injection beam-bump magnets, which operate with thyristor-controlled pulsed currents, were run at 50 Hz. The three extraction kicker magnets, which will run at 30 kV at 550 MeV beam energy, were also operated at 50 Hz. The heavy water cooling system for the depleted uranium target (200 kW of heat will be generated in the target at full performance) was successfully commissioned as were the cooling systems for the reflectors and the two ambient-temperature moderators. The control systems of the liquid hydrogen and liquid methane moderators were improved. The biological shield surrounding the target was completed and the beam line shutters put under central control.

Progressive commissioning of machine, target station and installed instruments began on 24 June and lasted until 9 September. During this time, the proton current increased to 10 μA at 550 MeV, this being achieved at 2.5×10^{12} ppp at 25 Hz but limited, as expected, by the voltage induced in the synchrotron RF cavities by the proton bunches. A complex feedback system was successfully commissioned which produced 5×10^{12} ppp at 550 MeV, 20% of the design figure.

It was clear from the June–September run that the energy stability of the injector and the extraction efficiency had to be improved to keep beam losses to an acceptable level for a long period of operation. This work is reported below. By November, about 90% of the protons injected at 70 MeV were impinging on the target at 550 MeV.

Injector

Experience during the past year has shown that the injector will require further development if it is to reach the desired level of reliability and performance. One unexpected problem occurred in the 665 keV accelerating column of the pre-injector which, at high beam duty cycles, suffered a high spark-down rate. Surprisingly, a major improvement to the vacuum pumping system had little effect but a modification to the column structure has been more successful, viz the installation of inserts in 13 of the column electrodes to improve shielding of the glass insulator rings. A more effective set of inserts is being manufactured.

Problems have also been experienced with spark breakdown in the linac accelerating cavities. Sparking across soldered joints on the drift-tubes (salvaged from the RAL Proton Linear Accelerator and now over 25 years old) has been a recurring problem. The spark-damaged joints have been successfully repaired in situ by electroplating using a manual brush-plating technique. A more practical method for the in-situ plating of all 136 joints is being investigated.

Energy instability of the injector beam has contributed to the variable performance of the synchrotron. To combat this, modifications have been introduced to improve the stability of the linac accelerator fields, but at the expense of increased susceptibility of the RF system to pick-up interference. Further development is continuing.

Synchrotron

Injection System

Very thin (0.25 μm) foils of alumina are used to convert the 70 MeV H^- ions from the injector into protons during the injection process. Equipment is being developed to replace damaged foils automatically. Foils are exchanged from a cassette holding up to 32 foils and the cassettes may be replaced without disturbing the synchrotron vacuum. The automatic foil exchange system is being prepared for testing under vacuum prior to installation.

Diagnostics

The diagnostic systems used to measure beam parameters have performed well. The parameters are beam intensity, position, profile and loss from the

Fig 4.1 Proton beam intensity during 10 ms acceleration period in the synchrotron, at 4 x 10^{11} protons per vertical division. High efficiency is shown by the large percentage of injected beam accelerated to 550 MeV.

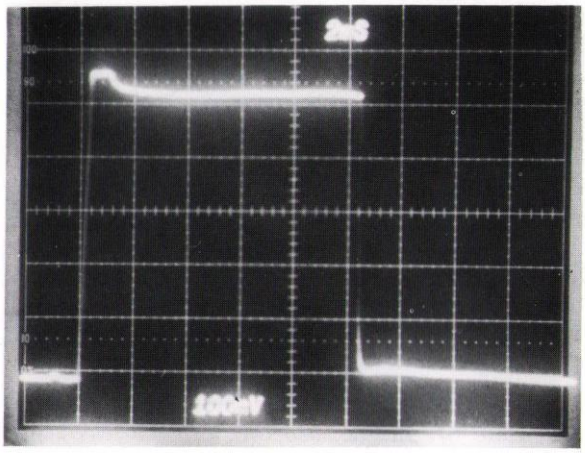

machine. Fig 4.1 shows the proton beam intensity during the 10msec acceleration period, and Fig 4.2 displays profiles of the beam at three positions in the extracted beam line as it is transported to the uranium target. Further diagnostic devices have been installed this year, including a multi-wire profile monitor to measure energy instability in the linac (Fig 4.3), a scintillator in the extracted proton beam line to monitor the beam shape and position as it is extracted from the synchrotron, and a beam pulse digitizer system to investigate the beam bunch shape during acceleration.

RF Acceleration System

The radiofrequency system with its four cavities has now operated for more than 4500 hours with very few failures. The main effort this year has been in the installation and commissioning of a beam loading compensation system. As the high-intensity beam bunches in the synchrotron pass through the accelerating cavities, they induce voltages which affect the accelerating voltage. The beam compensation system uses a signal from a beam intensity monitor to produce a current in the cavity equal and opposite to that produced by the beam. This requires variable wide-band electronic delays to match the delay through the RF system to the changing frequency of the beam. Use of the beam compensation system has allowed acceleration at beam intensities up to 5×10^{12} ppp, an increase by a factor 2, and the upper limit has not yet been reached. Future development of the RF system will include the installation of the two remaining RF cavities in 1986, and further development of the beam compensation system to produce performance at the design level.

Extraction System

Fast extraction of the two proton bunches is achieved via a dc extraction septum magnet, following the creation of a slow orbit bump and the pulsing of fast kicker magnets (Fig 4.4). The rise time of the kicker fields is 225nsec and the flat-top duration approximately 500nsec. The extracted beam may be observed at the input of the septum magnet as it intercepts a scintillation screen. The presence of the slow orbit bump has been found to introduce a halo on the circulating beam; four wings develop which may be reduced by adjusting the betatron tunes of the ring. At present intensities, the system may be adjusted to eliminate beam loss at extraction. The extraction system is shown in Plate X.

Remote Handling

As part of the process of introducing remote handling techniques into repair and modification of the synchrotron, two remotely-controlled arms have been mounted on the 45t radial crane and are now in use (Plate XI). One arm has 3 degrees of movement (radial, azimuthal and extension) and normally carries a radiation probe with remote reading of the associated

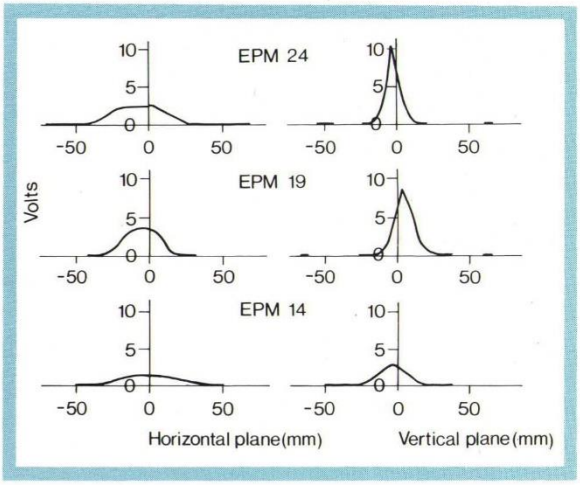

Fig 4.2 Profiles of the proton beam at 3 positions in the extracted beam line. EPM 14 and EPM 24 are 55m apart. The focusing effect of quadrupole magnets is shown at EPM 19.

control box via closed-circuit television. The other arm, capable of radial movement and extension only, carries another camera mounted on a pan/tilt unit. The azimuthal position of the crane is controlled from the main control room via a radio-frequency link, Position of the crane, relative to index marks on the synchrotron room walls, is monitored via the TV links. The system has been used to locate beam loss points (by finding local 'hot spots' of induced radioactivity) without the need to expose personnel to radiation or to spend time

Fig 4.3 Multi-wire profile monitor used in the proton extracted beam line. 48 signals/monitor are fed via complex electronic circuitry to a computer-controlled display. (85FC2206)

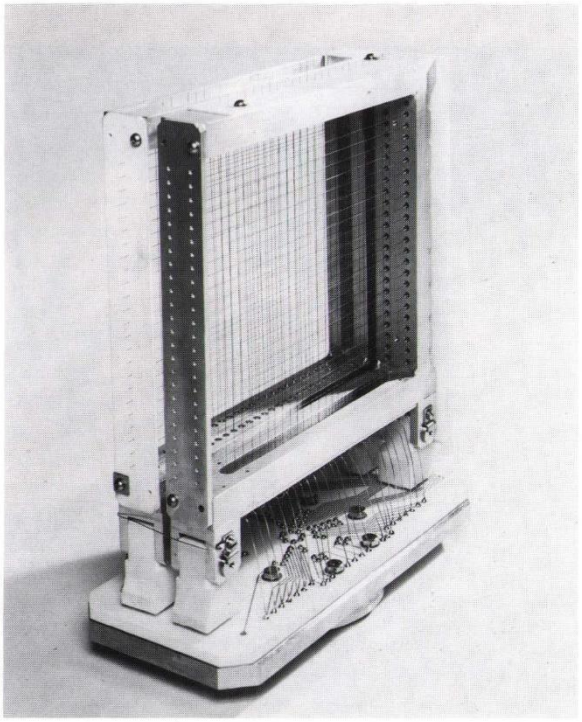

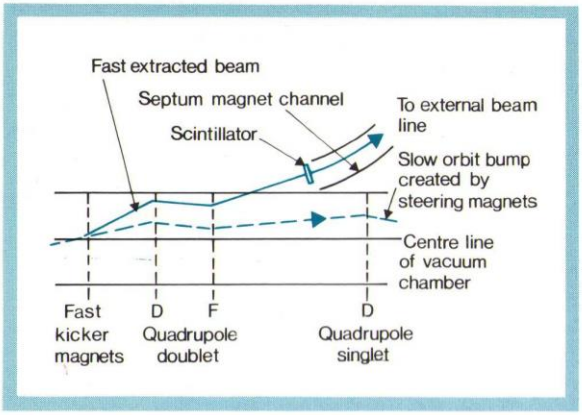

Fig 4.4 Schematic of vertical extraction of the proton beam from the synchrotron.

breaking and subsequently re-establishing interlock chains.

Target Station

Following the success of the low-intensity commissioning run in December 1984, the first half of 1985 was spent in intense activity to complete the installation and commissioning of the target station and its systems to the level required for routine operations at 10% design intensity.

Main Shielding

The installation of the permanent steel and concrete biological shielding was completed in May. The 18 shutters and associated shielding were installed and the first batch of lift systems were completed together with the electrical power control and monitoring to make them fully operational. During the first phase of commissioning in June, mechanical difficulties were encountered with the jacks which raise and lower the shutters. This resulted in the need to limit operation of the shutters until September when the problem was solved. Towards the end of September, the proton beam intensity reached 10μA, which allowed meaningful measurements of the performance of the shielding to be made. The leakage from the top of the shield, about 60μSv/h at most, confirmed the design calculations. At full intensity, the layer of concrete blocks above the shutters will be replaced by steel.

Target Moderator Reflector Assembly

The first assembly of the target moderator and reflector for the December 1984 run had highlighted some areas where mechanical improvements were required. The assembly was dismantled, modified and then reassembled in May. During the rebuild, the opportunity was taken to test the remote handling procedure for removing an irradiated target. The complete target assembly can be seen in the remote handling cell (Fig 4.5).

Much work was necessary to bring the cryogenics systems up to the standards required for routine operation, particularly the controls. The first cool-down of the moderators prior to experimental operation revealed heat leaks in both flexible cryogenic transfer lines in the highly-curved sections close to the target assembly. These heat leaks developed over the shut-down after December 1984. Modifications were

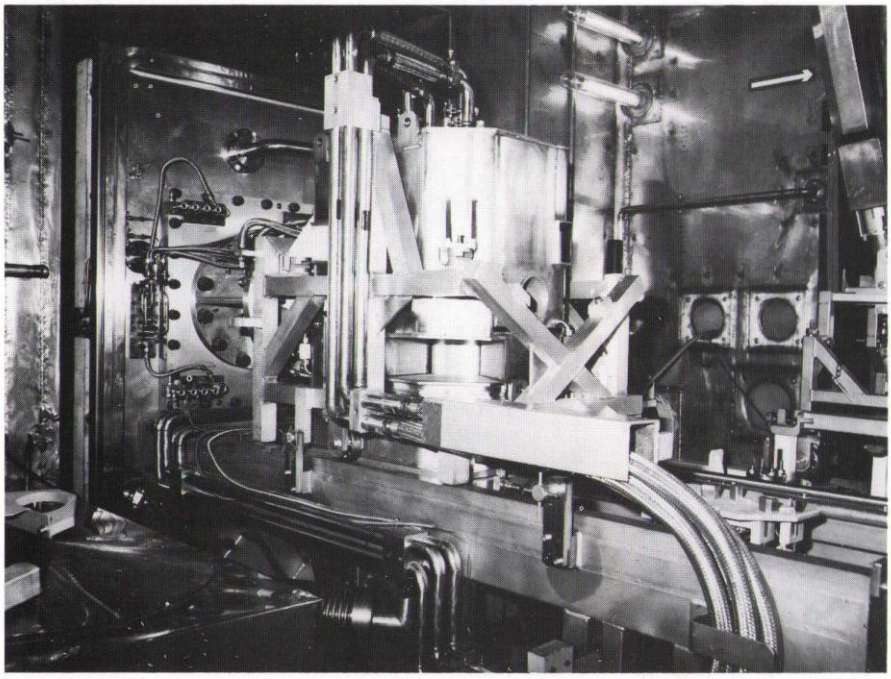

Fig 4.5 Target assembly in the remote handling cell. When installed in the target void vessel, protons enter the target through the hole on the right of the reflector vessel. In the cut-out towards the bottom of the assembly can be seen the face of the liquid methane moderator. (85RC2936)

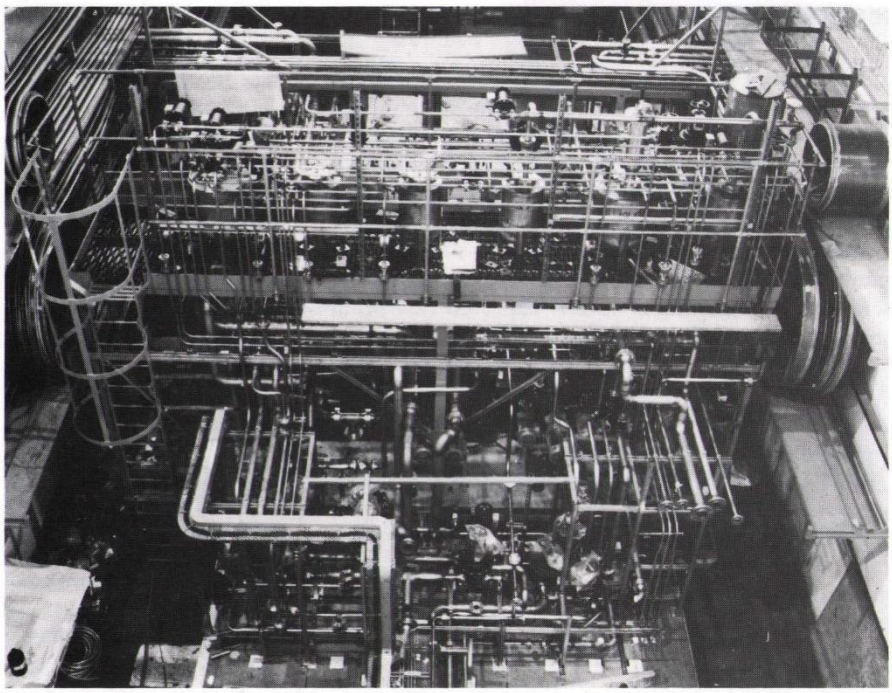

Fig 4.6 Part of the ISIS target station services area, showing heavy and light water cooling circuits for the target assembly on their mobile carriage. (85RC4789)

carried out in collaboration with the manufacturer and the systems were made operational in June. The available refrigeration is 1.1kW for the hydrogen and 0.7kW for the methane, both in excess of design. Operation of the moderators has been relatively trouble-free, with the methane at 100K, 4 bar, and hydrogen at 20K, 12 bar.

Water Cooling Systems

The water-cooling circuits (Fig 4.6) contain seven separate circuits, including 250 computer-controlled valves, pressure sensors, flowmeters and thermometers. Installation of the system was completed and commissioned by computer control in May. Initially, light water was used for target and reflector cooling to gain operational experience. The circuits behaved in an extremely predictable and stable manner and were drained and filled with heavy water in July. This involved operating several valves on the target assembly in the remote handling cell using the master-slave manipulators. This was the first occasion on which the manipulators had been used 'in anger' and the coolant change went very smoothly, a most encouraging start to remote handling operations.

Operational Experience

During the main period of operation from June to September, the target station system proved to be extremely reliable. The only major problem encountered was the mechanical difficulty with the shutters which was resolved. At the maximum current, 10μA, achieved during the year, the temperature of the target rose to 15°C above ambient, in good agreement with that expected (a 380°C rise is expected at the full current, 200μA).

The cryogenic systems behaved as expected with first indications of the production by radiolysis of higher hydrocarbons, mainly ethane, in the methane system. This manifested itself as an increase in pressure drop across filters in the circuit, which would be expected as the higher hydrocarbons have freezing points above the 100K operating temperature.

By November, nine beam holes were operational and the neutron fluxes from the moderators were broadly as expected. Further work is necessary to optimise the open positions of the shutters before a detailed comparison of absolute fluxes is possible over all energy ranges.

Control System

There are now over 1000 control programs on the four control computers. Enhancements to the system include software to centralise control in the main control room, an additional disk drive on one computer and the inclusion of a fast transient digitizer. Further extensions of the control console are planned. Re-arrangement of computer interface branches has resulted in improved response times, in particular for beam diagnostic data acquisition. A further 60 interface modules have been produced to cater for additional requirements, and a multi-interrupt module has been developed to facilitate alarm-handling.

NEUTRON BEAM RESEARCH

Services

There has been a successful conversion from the use of soft water and biocide treatment in the evaporation cooling towers to direct chemical treatment of water from the public supply to prevent the formation of scale, inhibit corrosion and restrict the growth of micro-organisms. The installation of absolute filters and a high-velocity air discharge chimney in the air-conditioning plant has been completed to cope with the increased air activation levels expected as beam intensity rises.

Neutron Scattering Programme

The first six months of operation of ISIS as a neutron scattering facility saw proton currents rise from 0.1 μA in June to 15 μA at the end of the year. Neutron production increased from 20 μA-hr in the first 2 week cycle to 400 μA-hr in the last cycle of the year. While these levels are modest in comparison with full intensity, which will give 200 μA-hr per hour, they have enabled the nine installed instruments to be commissioned and have produced many new scientific results.

A brief summary follows of what has been achieved over the last year on each of the instruments so far commissioned.

HRPD: High-Resolution Powder Diffractometer

Over the past twenty years, neutron powder diffraction has become established as an important and powerful technique in the elucidation of crystal structures but the resolution of neighbouring diffraction peaks on current instruments has limited the scientific possibilities. HRPD, as the first of a new generation of ultra-high resolution machines, has been designed to give an improvement in resolution of a factor 5–7 over existing diffractometers. Early experience on HRPD has shown that the instrument has opened up new areas and will considerably extend the power of the powder diffraction technique in both academic and industrial research.

The achievement of the substantial increase in resolution is illustrated in Fig 4.7 where diffraction data of an international standard sample of alumina (Al_2O_3) obtained on HRPD and at Argonne National Laboratory are compared. Numerous previously unresolved peaks are split in the HRPD data and a far higher degree of lattice parameter precision has been obtained (HRPD Al_2O_3 data: a = 4.75998(2) Å; c = 12.99883(4) Å). This corresponds to an accuracy of a few parts in 10^6 and is comparable with the very best single-crystal X-ray data (a = 4.75999(3) Å; c = 12.99481(7) Å). Similarly, for rhombohedral NiO, the angular distortion from cubic symmetry has been measured to be 90.05943(7)°; this precision bodes well for detailed structural studies of phase transitions. Indeed, detailed peak-shape analyses of the powder-diffraction profiles have confirmed the anticipated instrumental resolution but, additionally, in every profile investigated to date, have revealed significant sample-broadening effects. For Al_2O_3, for instance, the least-squares fitting of a peak shape (a convolution of

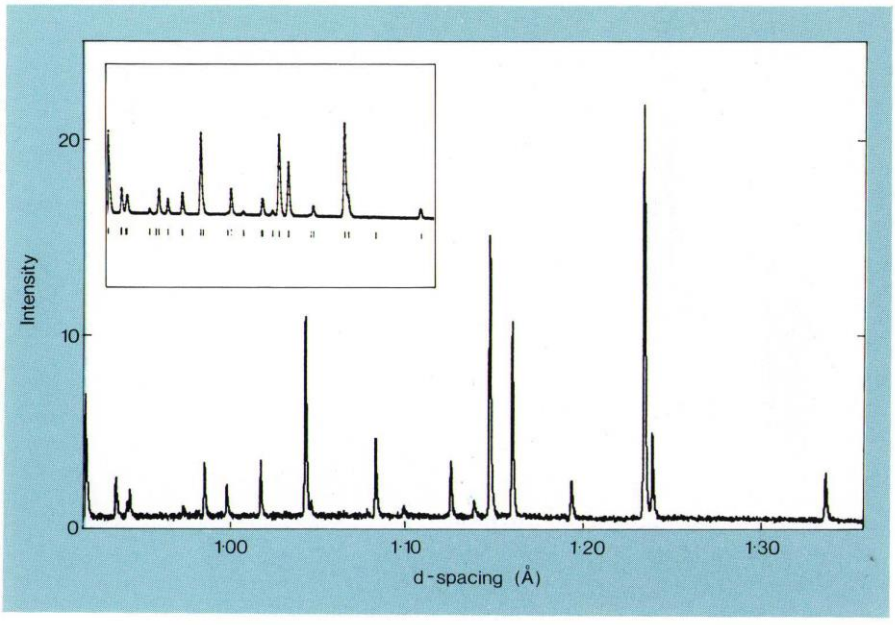

Fig 4.7 Comparison of the powder diffraction pattern of the standard Al_2O_3 measured on HRPD with the previous best resolution data from IPNS (insert).

exponential, Gaussian and Lorentzian functions) to data taken at high d-spacing indicated that sample broadening was present and could be attributed to an average crystallite size of 2.2μm.

Many academically and industrially important materials either cannot be synthesised or can only be synthesised at great cost as single crystals. This often places significant limitations on the ability to understand and characterise such substances. The most fundamental and serious setback to date in this respect has been the virtual impossibility to determine directly unknown structures of powder samples. The current state of the art is that structural models with more than 100 variable parameters can be refined, but the determination of structures from powder data has remained an empirical rather than an exact art. This is because existing diffractometers have inadequate resolution to resolve a sufficient number of individual peaks and unravel the necessary diffraction details.

The determination of a structure, whether from single crystal or powder data, can best be understood in terms of four discrete steps: indexing of the powder pattern and determination of the crystal system and lattice parameters; identification of the space group; solution of the phase problem and determination of an approximate structure; refinement of the structure.

Preliminary analysis of the neutron powder diffraction pattern (Fig 4.8) of $FeAsO_4$ recorded on HRPD clearly indicated that $FeAsO_4$ possessed a complex crystal structure of low symmetry. Auto-indexing of the 20 highest d-spacing reflections using the VISSER program proceeded routinely and gave monoclinic cell dimensions: a = 7.563(1)Å, b = 8.0795(1)Å, c = 5.0117(1)Å, β = 10.447(1)°. With this information, all 83 highest d-spacing peaks were indexed; systematic absences implied space group symmetry $P2_1/n$. A further 56 systematically-present but unobserved reflections were assigned small non-zero intensities and the resultant 139 reflections were then used to provide |F(hkl)| values for the structure-solving direct methods program MITHRIL. Both triplets and negative quartets were calculated and yielded approximate atomic positions which corresponded to a chemically reasonable solution. These approximate parameters were then refined by an integrated intensities least-squares procedure (GRILS) based upon the Cambridge

Fig 4.8 Time-of-flight neutron powder diffraction pattern for $FeAsO_4$ prior to normalisation. Inset: the [001] projection of the crystal structure derived using auto-indexing and single crystal direct methods. The complex monoclinic structure was obtained using triplets and negative quartets in the direct methods package MITHRIL and consists of tetrahedrally coordinated arsenic and edge-shared 5-coordinated iron ions.

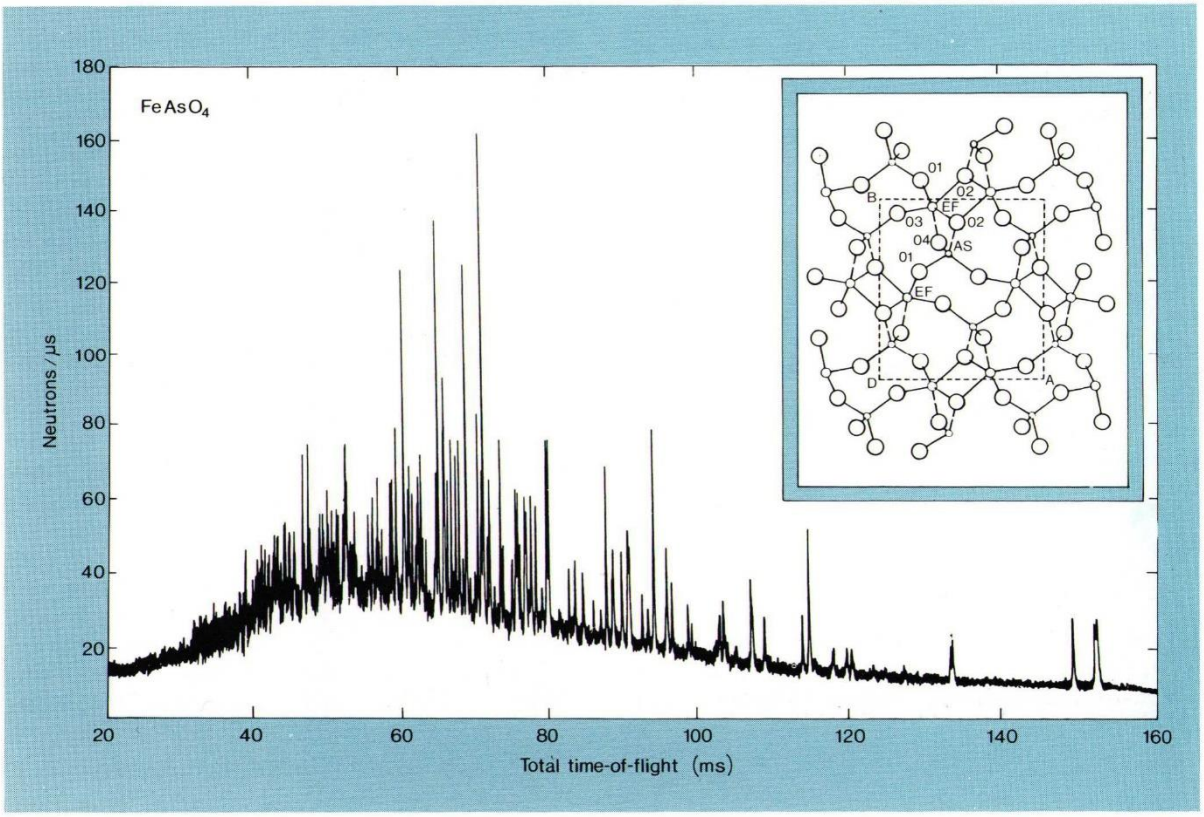

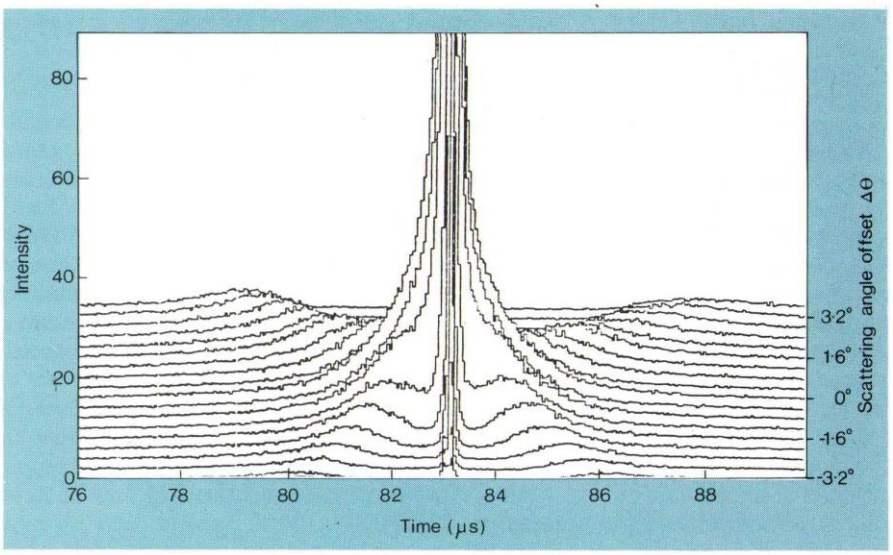

Fig 4.9 (004) reflection from pyrolytic graphite measured on HRPD as a function of time of flight and scattering angle offset $\Delta\theta$ from the Bragg angle.

Crystallographic Subroutine Library. The final structure illustrated in Fig 4.8 (inset) contains five-coordinated ion atoms, with approximately edge-shared trigonal bipyramidal stereochemistry, which are linked via shared oxygen atoms to tetrahedal AsO_4 units.

HRPD, with its position-sensitive detector, represents a significant advance in instrumentation. It allows, for example, novel experiments to be performed such as the study of one-phonon scattering surfaces of pyrolytic graphite. The scattering pattern in Fig 4.9 clearly shows four wings radiating from the base of the 004 Bragg peak from PG. These are manifestations of the hyperbolic one-phonon acoustic scattering surfaces present when the neutron velocity exceeds the sound velocity in the crystal. Analysis of the data gives the velocity of sound perpendicular to the lattice planes in agreement with accepted values. This is a general method of determining sound velocities in crystals without the drawbacks of transducer techniques, and

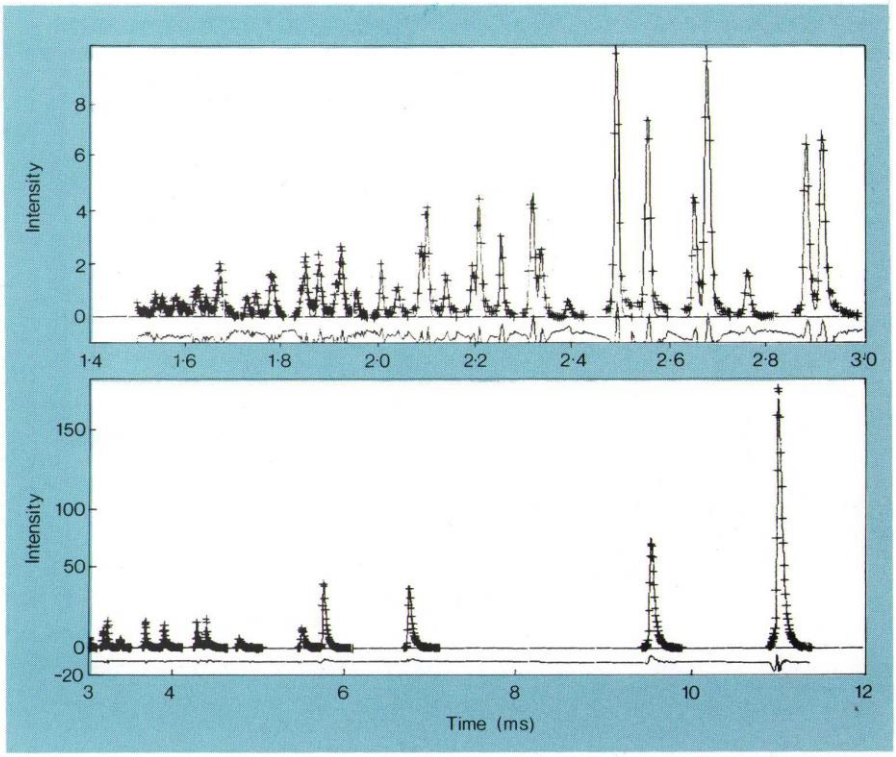

Fig 4.10 Observed (crosses), calculated (full line) and difference profile plots for nickel metal. The diffraction peaks were fitted to a Gaussian-double exponential peak shape function, representing the predicted decay constants for epithermal and thermal neutrons convolved with a geometrical term. The excellent profile fit is reflected in the low powder profile.

promises to be of particular value for measurements under extreme conditions of temperature and pressure.

The first forty days of neutrons on HRPD have been divided between calibration experiments and novel research in collaboration with university scientists. Because of the innovative nature of the detectors, electronics and computer software, instrument commissioning and calibration have been important in verifying the predicted design characteristics of HRPD and in assessing the performance of new high-technology components. With commissioning almost completed and the first university experiments successfully undertaken, all new components and instrument predictions have been validated. The software to support the powder diffraction facilities continues to be developed. In particular, the first full profile analyses using code written at RAL have been successfully performed on Ni (Fig 4.10), TiO_2 and Al_2O_3 data.

LAD: Liquids and Amorphous Diffractometer

The first half of the operating period was taken up with calibration experiments. With the time-of-flight technique, determination of distances, scattering angles and other instrumental parameters is of utmost importance in order to provide accurate conversion of time to wavelength and Q-vector ($Q = 4\pi\sin\theta/\lambda$). This is most critical at short wavelengths. Foils of metals such as uranium and iridium which have well-defined absorption resonances have therefore been used to give distances and to calibrate the high energy region. A standard powder such as nickel was used to determine the scattering angles of the detectors and to measure the shape and width of the resolution function. Measurements of the background show that energies up to 25 eV (0.06 Å) are accessible at all scattering angles and 100 eV (0.03 Å) at some. This means that high Q-values are available even at low scattering angles where the inelasticity corrections are small.

During the second half of the operating period, the first liquid and amorphous samples were measured. The static structure S(Q) of vitreous silica has been extensively studied on reactor-based diffractometers and was thus an ideal first sample to test the performance of LAD. The sample measuring time was 200 μA-hr corresponding to one hour at full ISIS intensity and preliminary analysis shows that the results, though not as good statistically, agree well with the reactor data up to $Q \approx 24\,Å^{-1}$ which represents the maximum momentum transfer for D4 at ILL. With the LAD data, however, oscillations in the S(Q) up to $Q \approx 40\,Å^{-1}$ are still evident and the data extend well beyond $100\,Å^{-1}$ (Fig 4.11a). This wider Q-range then has the advantage that, when the data are Fourier transformed to the radial distribution function g(r) (Fig 4.11b), the resolution of the main peaks is twice as good as that of the equivalent reactor data.

A short test run on PTFE provided some unexpected

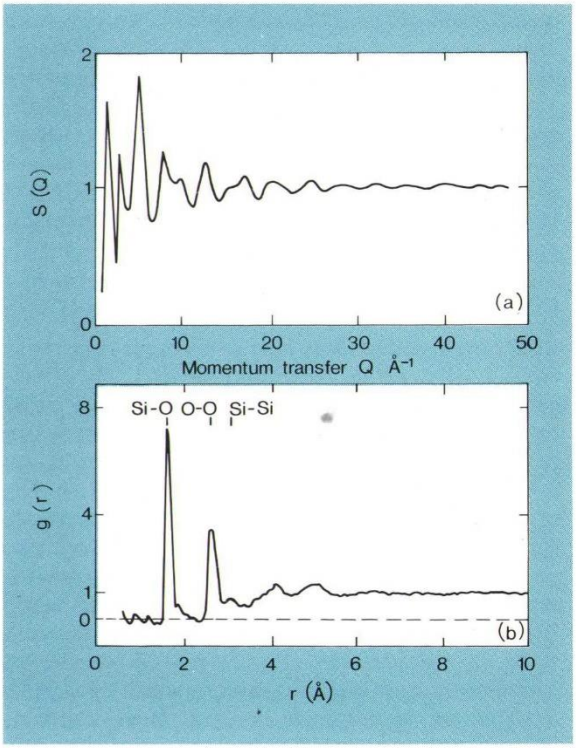

Fig 4.11 a) Structure factor S(Q) for silica measured on LAD combining data at 150° and 20° scattering angle. b) Radial distribution function g(r) for silica obtained from the S(Q) data of (a). Nearest interatomic distances are indicated.

but extremely useful information on the effects of resolution. The data on LAD at high scattering angles have a sharp peak at $Q \approx 1.2\,Å^{-1}$, a feature which has not been observed on reactor instrumentation. The resolution of LAD deteriorates with decreasing scattering angles so that, as the angle decreases, the sharp peak broadens and decreases in height until at 10° the feature is lost.

SXD: Single-Crystal Diffractometer

SXD detected its first neutrons in November. Initial measurements have been made using a single ($20 \times 20\,mm^2$) scintillator detector to determine the time structure of single crystal diffraction data. The detector was then masked and the spot shapes and extents in detector space were measured. These data have provided sufficient information for complete preliminary parametrisation of the 3D shape of reflections to be made, and these results will be incorporated into the data reduction programs which are under development.

An Anger camera position-sensitive detector under development for SXD has been built and is currently being tested. This uses an array of 45 hexagonal phototubes and is designed to give a spatial resolution of approximately 2–3 mm. The dimensions of the Anger camera are 300×300 mm and it is envisaged that, in full working mode, an array of 128×128

spatial pixels will be used, with up to 700 time channels, binned in widths of constant dt/t. The sheer volume of data thus produced poses a daunting data-processing problem. SXD will use the original PUNCH HUB computer, a VAX 11/750 giving over 400 Mbyte of disk space, and it is expected that on-line data reduction will enable analysis of a complete set of PSD data ($128 \times 128 \times 700$) in around 20–30 minutes when ISIS operates at full intensity.

LOQ: Low-Q Diffractometer

LOQ is designed to study long range order in materials, typically for scattering from particles or inhomogeneities on a scale of 10 to 500 Å. Samples include biological specimens such as proteins or viruses, polymers, metal alloys, porous solids, colloids and other novel and exotic materials. Such a diverse range of systems requires an extremely flexible apparatus, the components of which have been installed and made operational this year. By mid-summer, neutrons reached the prototype detector segment temporarily fixed in its large vacuum tank. Following this milestone, a considerable effort was still required to complete the interior of the tank, to make the detector movable and to finish the incident beam line which includes two mechanical choppers for neutron wavelength selection. Initial results from the 560-element glass scintillator detector array are promising and a second 40° segment is being built. This will increase the count rate and allow studies of anisotropic or oriented samples such as fibres.

HET: High Energy Transfer Spectrometer

HET has been successfully commissioned and preliminary experiments on the vibrational modes of hydrogenous systems and crystal field transitions have been performed. The spectrometer is designed to study high-energy inelastic excitations, particularly with low associated momentum transfer. It uses a fast (1 μs burst time) fermi chopper spinning at 600 Hz as its monochromating device. No problems were experienced in phasing the chopper to the source (or rather the source to the chopper!). Incident energies were easily changed by rephasing the chopper, and different energy ranges could be selected by operating at a different multiple of the source frequency. The predicted value of the resolution of the elastic line ($\Delta E_i/E_i \sim 0.8\%$) has been confirmed by measurement and an inelastic feature in solid formic acid at 171 meV transfer was observed with a FWHM of 2.6 meV, corresponding to the expected value from an incident energy of 250 meV.

The full complement of low angle (3°–7°) gas detectors was installed but only a test octant of the 9°–30° scintillator bank. Although these detectors achieved their specification for intrinsic background and γ sensitivity, problems were experienced with γ-rays associated with losses in the extracted proton beam line and in observing very weak inelastic features which were clearly seen in the gas detectors. As a consequence, the decision has been made to use gas detectors at all scattering angles.

Although it is anticipated that at least 500 μA-hr

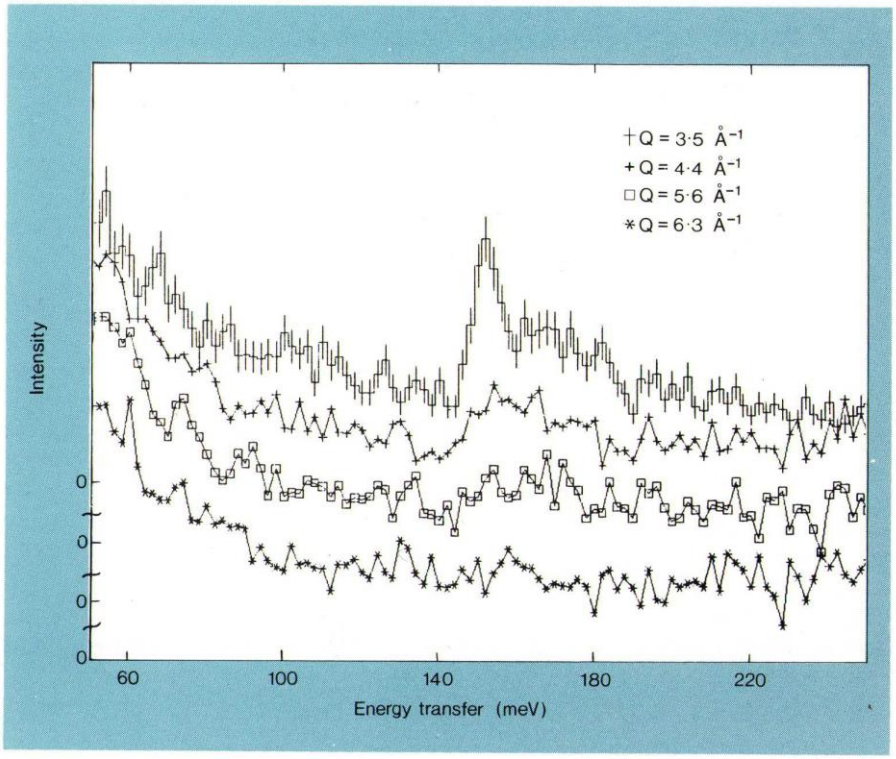

Fig 4.12 Inelastic scattering from UO_2 measured on HET. The $\Gamma_5 \rightarrow \Gamma_3$ crystal field transition at 155 meV decreases in intensity with increasing Q, confirming its magnetic origin. The origin of the structure on the high energy side of this peak is under investigation in collaboration with Oxford University at Harwell.

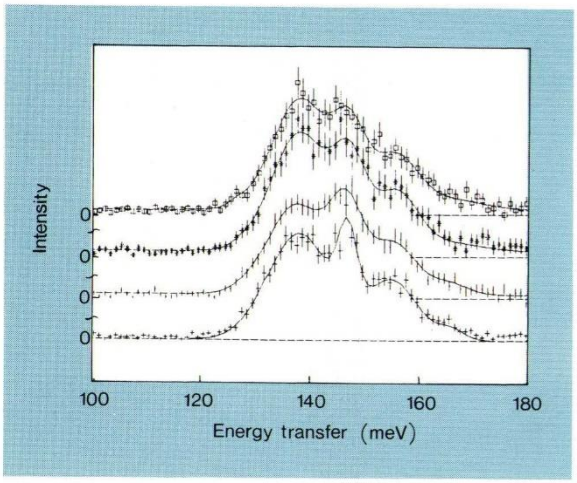

Fig 4.13 Internal structure of the fundamental mode of ZrH_2 as measured on HET as a function of momentum transfer, Q, ranging from 4.0 to 5.5 $Å^{-1}$.

running will be required to obtain good inelastic data, preliminary investigations of the vibrational spectroscopy of hydrogen-bonded systems and metal hydrides have been performed and crystal field transitions in UO_2 observed (Fig 4.12). A study of formic acid by Durham University has already shown how the high resolution and low momentum transfer can be used to investigate previously unresolved features in the spectrum. The quality of data from this spectrometer is such that systems like ZrH_2, long used as a standard in inelastic neutron scattering, now reveal a complexity previously only hinted at. Fig 4.13 shows the momentum transfer dependence of the three clearly-resolved components in the fundamental mode of this system which was long thought to be an isotropic single harmonic oscillator. Complementary data taken with good resolution but at higher momentum transfer from TFXA are shown in Fig 4.14.

TFXA: Time-Focused Crystal Analyser

Installation of TFXA is complete, and the first half of the analyser/detector solid angle has been fully commissioned. Commissioning of the remaining analyser/detector solid angle was completed in November, and a full user programme commenced in December. The performance of TFXA is most encouraging. The count rates obtained lie within a factor 2 of theoretical estimates. The width of the elastic line is 0.3 meV, and the resolution is of the order of 2 to 3% over a wide range of energy transfers, confirming earlier calculations. Of particular note is the excellent signal to noise ratio measured for the samples used during commissioning, namely zirconium hydride and potassium hydrogen maleate, Figs 4.14 and 4.15. Data reduction software is well advanced, and users

Fig 4.14 Inelastic neutron scattering spectrum of ZrH_2 as measured by TFXA.

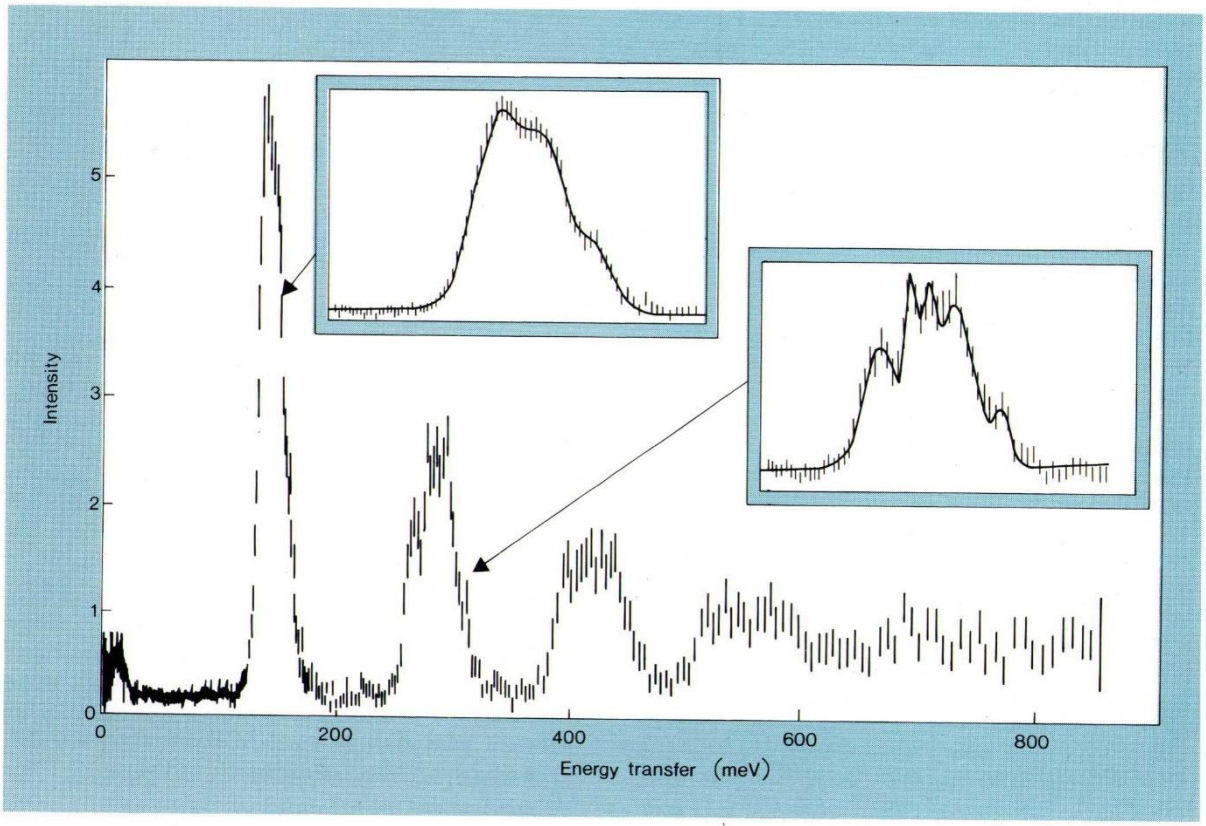

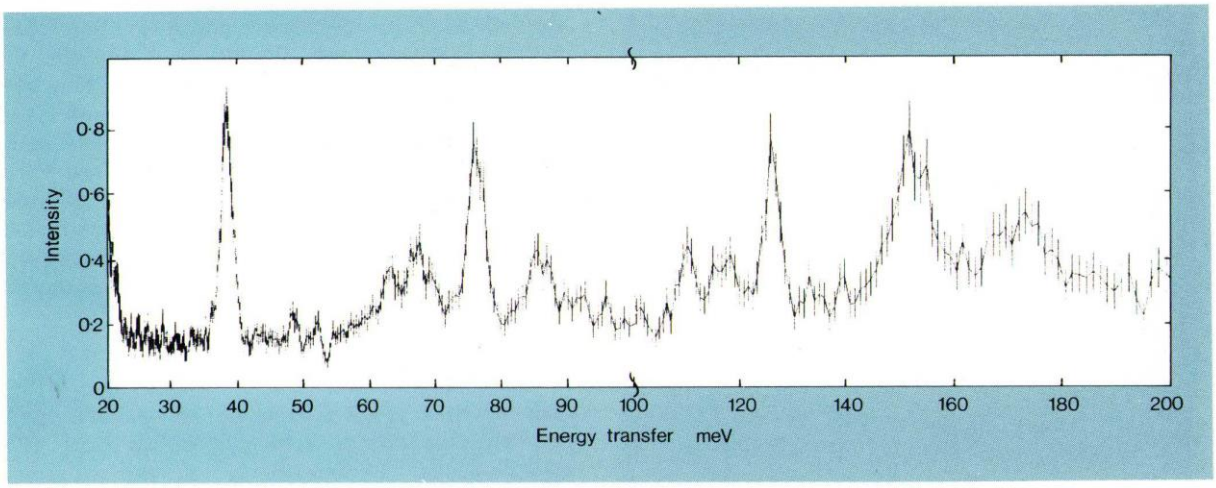

Fig 4.15 Inelastic neutron scattering spectrum of potassium hydrogen maleate measured at 2% resolution by TFXA.

can obtain normalised data proportional to cross section or scattering law using standard procedures.

A refinable normal coordinate analysis program developed at ILL has been extended to include powder averaging, overtones and combinations, and is now available at RAL. The potassium hydrogen maleate data are currently being analysed using this program.

Recent Monte Carlo calculations suggest that increases in count rate can be made by improvements to the analyser crystals: these improvements will be tested shortly. Calculations on the effects of multiple scattering on TFXA are in progress. Preliminary findings suggest that the use of thicker samples is feasible giving a significant increase in data rate.

IRIS: High-Resolution Inelastic Spectrometer

IRIS is an inverse geometry spectrometer designed for the study of diffusional and reorientational atomic and molecular motions which occur on timescales of 10^{-9} to 10^{-12}s. The beryllium-beryllium window analyser, provided by Bhabha Atomic Research Centre, is the first of three possible analyser systems to be installed on the IRIS beam line and was commissioned during the year. The window analyser is situated at the end of a 30m nickel-plated glass guide. The measured throughput of the guide tends towards 70% at the longer wavelengths, in good agreement with the calculated performance. The peak intensity is between 4Å and 5Å and the guide continues to transmit neutrons down to 1.5Å, but few neutrons are transmitted below this wavelength, indicating the guide's effectiveness as a low band pass filter. The characteristic wavelength of the guide is 3.5Å and the intensity at this wavelength is 2/3 of the plateau intensity as predicted by theory.

The frame overlap disc chopper, situated at 6.4m from the moderator, operates routinely at 50Hz with a phase stability of $\pm 10\mu$s. The wavelength band of 2.4Å passed by the chopper is within the frame overlap condition at the analyser position. The chopper can be easily rephased with respect to the ISIS extraction pulses, thus allowing this wavelength band to be selected from a wavelength range between 2 and 15Å. The energy resolution of the spectrometer, measured using a 30% scattering ZrH_2 sample, is 255μeV over the whole of the accessible Q range. The observed elastic peak intensity is in agreement with theoretical predictions and the signal to noise ratio is 20:1.

The overall performance of the spectrometer has been investigated using a sample of NH_4Br which undergoes a phase transition from an ordered to a disordered phase at 235K. Measurements were made at room temperature in the disordered plastic phase and the observed quasielastic broadening could be fitted with a model scattering law corresponding to reorientation of the ammonium ion about the three C_4 cubic axes (plus an inversion centre) with a relaxation time $\tau_1 \sim 10^{-11}$s. Data from this demonstration experiment are shown in Fig 4.16.

POLARIS: Polarised Neutron Spectrometer

At present, POLARIS is used as a high-count rate powder diffractometer with a polarised neutron option. There are 18 detectors with a $\Delta Q/Q$ resolution ranging between 0.6% on the backward angle (14.5°) and 10% on the forward angle (12°). The sample tank and detectors are contained inside a blockhouse to allow easy access to the sample area. This arrangement also allows great flexibility so that the instrument can be easily modified in the light of future development work.

A major use of the beam line has been the commissioning of the polarising filter. Polarising devices which operate over a broad energy range are essential for efficient utilisation of a pulsed neutron source. One such device is a filter containing aligned nuclei of ^{149}Sm. This will preferentially absorb one neutron spin state

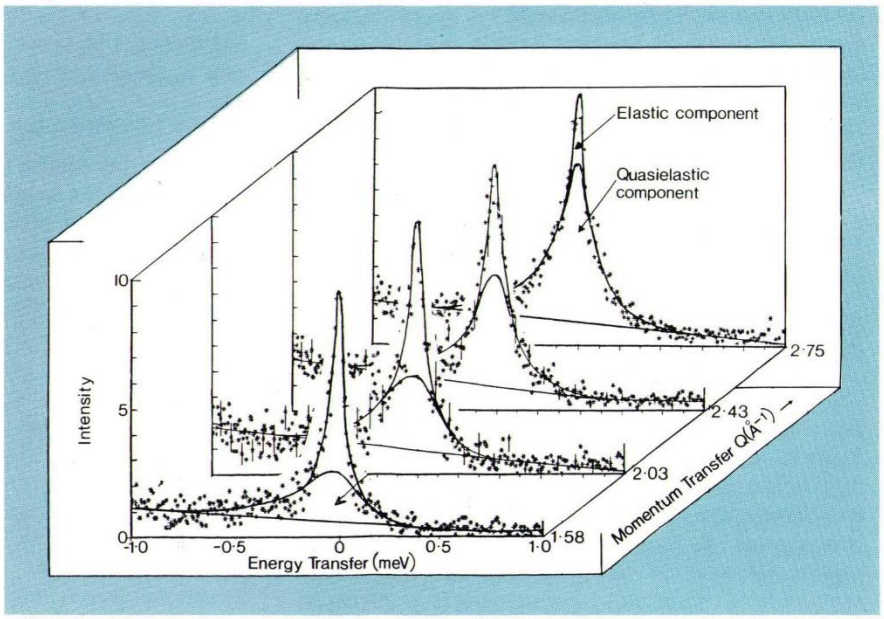

Fig 4.16 Quasielastic neutron scattering from reorientational mode of the NH_4^+ ions in ammonium bromide measured on IRIS. The reorientational jump rate is 25 GHz at room temperature.

over a broad energy range around the 98 meV resonance absorption peak. The nuclei must be aligned in a magnetic field at temperatures of ~0.01 K. The most recent prototype filter tested on ISIS consisted of a thin sheet (0.2 mm) of sintered $SmCo_5$, cooled to 0.015 K in a dilution refrigerator. A minimum beam polarisation of 80% was achieved over the entire range of neutron energies below 140 meV. At the resonance absorption peak the polarisation was better than 99% with a transmittance of 12%. This filter is the first produced anywhere in the world with a performance sufficient to make it a viable component of a polarised thermal neutron instrument. The tests also showed that the dilution refrigerator would operate satisfactorily for extended periods as a beam line component.

eVS: Electron-Volt Spectrometer

eVS has been built as a versatile development instrument incorporating improved versions of the (n,γ) resonance detector system originally used on the Harwell linac and a resonance filter difference system developed in collaboration with Los Alamos National Laboratory. The initial goal is a thorough evaluation of both techniques in the fields of high-energy low momentum transfer excitations (such as those found in magnetic systems) and high-energy recoil experiments on light atoms. Central to the instrument is the incorporation of a low albedo collimation designed to minimise off-energy contamination of a well-defined beam. The instrument was commissioned in late summer and excellent beam quality has been observed up to 200 eV.

General Performance

Measurements of the absolute neutronic performance of the ISIS moderators were made last December. These data are now fully analysed, and show excellent agreement with the design specification. Analysis of the neutron pulse shapes for various moderators has been carried out and again excellent accord with the design has been found. Shutter and collimation systems have all performed well as have the cold and thermal neutron guides. No biological radiation problems have been encountered and instrumental shielding has proved so effective that 'intrinsic' background levels are recorded by the detectors a few hundred micro-seconds after the proton pulse.

Support of ISIS Experimental Facilities

Computing

This year has included the successful installation and operation of six new instrument systems (bringing to nine the total number of working instrument systems), the delivery of the new HUB computer (VAX 8600), and the development of a new high-level data analysis language (GENIE).

The plans for the ISIS computer system (PUNCH) have always included provision for a large super-mini to act as the central component in the ISIS data analysis and archival system. With the announcement in 1984 of the VAX 8600, a 4.5 MIP machine capable of supporting many tens of users, it became possible to implement these plans with a machine compatible with the existing PUNCH computers. The VAX 8600 was delivered in September and installed in three days. The configuration includes 12 Mb of memory, 1700 Mb of disk storage, three magnetic tape drives and links to both the PUNCH local area network and the JANET wide area network.

GENIE is a new language for the manipulation and display of spectra. It has been written to enable all the ISIS instruments to use common software for the first stages of neutron data analysis and display. The features that take it beyond existing analysis and display software are flow control, algebraic manipulation and the ability to call external programs in real time. It is already extensively used on all instruments and will undoubtedly spread to many other applications where spectra manipulations are involved.

Operations, Sample Environment and Sample Preparation

The advantages of standardisation of the sample environment equipment have already been demonstrated: the standard panels for electrical and mechanical services have proved highly successful as have the computer-controlled closed-cycle refrigerators. A furnace is under construction which will be capable of reaching 1800°C, taking three samples at a time and allowing sample changing at temperature and under vacuum. The 10 kbar helium pressure unit has been refurbished for use on an experiment to study ice. Some cryostats have been modified to take vanadium 'tails'. A range of sample holders and fittings has been made. The main parts of a goniometer for room temperature operation have been delivered. A laboratory with fume cupboards and glove box has been refurbished and provided with chemicals and equipment for sample preparation. An operations group has been formed to carry out routine maintenance and repairs to instruments and equipment and to install sample environment equipment.

Fig 4.17 Scintillator array for an ISIS neutron beam monitor.

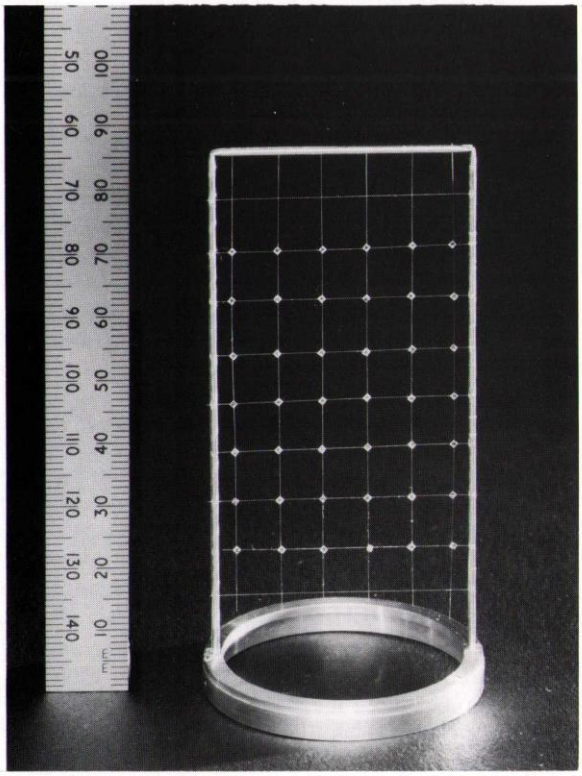

Detector Development

An improved version of the scintillator beam monitor counter has been developed and used successfully on all the ISIS neutron beam lines. Small pieces of lithium glass scintillator (approximately 0.25 mm cubes) are cemented on to an array of 50 μm diameter glass fibres. The spacing of the fibres and the number of scintillator pieces per fibre can be varied to change the efficiency of the monitor. The assembly is placed inside an aluminium foil reflector and viewed by an end-windowed photomultiplier as shown in Fig 4.17. The result is a monitor which presents very little scattering material to the beam, has a low efficiency ($10^{-4} - 10^{-5}$) to avoid saturation effects, and whose efficiency is a smooth function of neutron energy, thus avoiding difficulties caused by resonances in the traditional fission counter. The cylindrical housing can easily be put through a seal and the monitor used in vacuum. The very small size of the scintillator pieces means that secondary electrons produced by interaction with γ-rays escape before they deposit much energy. The resulting low photomultiplier output pulse height is well below a discriminator level set for neutron detection. The monitors can be used in the main neutron beam with no problems from γ sensitivity. The pulse height spectrum produced by neutron detection shows a well-defined peak which makes for good discrimination and stable operation.

Another detector working on the same principle has been used to scan the incident neutron beam on a number of instruments to check the quality of the collimation and to measure the beam size and position at the sample. This device uses a single glass fibre to which small scintillator pieces are cemented, again contained in an aluminium foil reflector and viewed by an end-windowed photomultiplier. It is mounted on an arm which can be rotated in vacuum about a vertical axis so that the detector scans the beam in the horizontal plane. The HET and IRIS beams are the first two to be studied and excellent results have been obtained showing good collimation (low intensity penumbra on the beams) and good beam alignment.

Neutron Choppers

In addition to their use as a monochromator on HET, neutron choppers are essential components of several ISIS instruments as wavelength-limiting devices and for suppressing instrumental background. The HET fast fermi chopper has operated without problems on its KFA/IVG magnetic bearings for six months at frequencies of 600 Hz and 400 Hz. The HRPD three-aperture double-disc chopper and the single disc frame overlap chopper have performed well with open to closed transmission greater than 10^4 and 95% stability of ±10 μs with maximum excursions of ±30 μs. The

IRIS single fixed-aperture disc has also performed satisfactorily. Work is in progress to make the IRIS and three LOQ choppers operational as double disc variable-aperture devices by early 1986. A nimonic blade background suppressing chopper has performed well in laboratory tests and will be installed on HET in 1986.

X-ray Diffraction Facilities

An X-ray diffraction laboratory has been set up, centred around the use of a Multi-Wire Proportional Counter (MWPC) two-dimensional X-ray detector system developed at RAL. An X-ray powder diffractometer is currently being commissioned. These facilities are intended to give additional support to university users to complement the neutron scattering at ISIS. Development of the MWPC system is being pursued and a collaboration with Imperial College has adapted the MWPC diffractometer to allow small-angle scattering measurements to be carried out in the 20–500 Å d-spacing range.

Future Developments

Pulsed Muon Facility

A surface muon beam facility is being built in collaboration with France, Germany and Italy, under the umbrella of the European Commission stimulation programme, for research in solid state physics and chemistry using the muon spin resonance (μSR) technique. In the first instance the facility will comprise a thin muon-producing target located in the ISIS extracted proton beam, a muon transport beamline, and a μSR spectrometer with associated data acquisition systems. Even within the context of this development project, the facility will be the world's premier pulsed muon facility and provide unique opportunities for new research.

Design work has continued during the year, and major installation work will be carried out during the spring shutdown with the aim of producing a usable muon beam in the second half of 1986. A redesign of the beam line has produced a number of advantages: doubled muon intensity; simplified channel tuning; more symmetrical beam spot at sample position; improved shielding.

Work directed towards the choice of μSR spectrometer has continued in collaboration with scientists from Italy, Japan and Sweden. The huge anticipated flux of incident muons and their decay positrons necessitates division of the positron detector into many segments so that, individually, they are not saturated. For each segment, the data-acquisition system resembles that for neutron time-of-flight spectra, but with the frame length compressed to the microsecond timescale characteristic of μSR. Technical options for the muon lifetime measurement and the transfer of data are presently being evaluated. In addition, attention is being given to μSR and cross-relaxation techniques which offer the possibility of a uniquely powerful facility.

CRISP: a Pulsed Source Neutron Reflectometer for Surface Studies

A time-of-flight neutron reflectometer has been designed and will be available for initial evaluation in mid-1986. Its applications cover a broad range of surface science including chemical interfacial phenomena, surface magnetism and low-dimensional structures. To investigate liquid surfaces, the instrument geometry incorporates an inclined incident beam (approximately 1.5° to the horizontal) and collimation providing a horizontal slit. A polarising supermirror will extend the technique to a polarised beam mode, which is essential for magnetic studies. A wide range in $(\sin\theta)/\lambda$ varying from 0.001 to 0.052 $Å^{-1}$ will be accessible at fixed geometry using wavelengths from 0.5 to 26 Å. Resolution will be in the range 2–10%.

PRISMA

A coherent inelastic spectrometer (PRISMA) will be installed on ISIS during 1986 under an international collaboration signed this year between SERC and CNR, Italy. The spectrometer will have 16 independent crystal analysers and detectors which will utilise the pulsed nature of the neutron beam to measure large regions of the phonon dispersion curves simultaneously without movement of the sample crystal. It will be particularly powerful in probing high-energy optical phonon branches which are notoriously difficult to measure using presently available instruments.

IRIS

The quasielastic spectrometer IRIS is presently equipped with beryllium analysers which provide an energy resolution of 50 μeV. The next phase of the spectrometer will be the installation of an array of 1320 pyrolytic graphite analysers and a position sensitive detector. Resolutions of 14 μeV will then be possible. The large solid angle of the analyser will enable data to be collected simultaneously over the complete range of scattering angles from 15° to 165°. Commissioning is planned for completion by October 1986.

Support Activities

The University Liaison Secretariat supports UK university and polytechnic scientists participating in neutron scattering programmes sponsored by SERC in the UK and overseas. It provides assistance with travel and accommodation, subsistence, supply of materials and equipment and helps to coordinate the programmes. Over 400 university staff, Research

NEUTRON BEAM RESEARCH

Associates and students are currently involved. A total of 426 proposals were submitted during the year; 302 were approved, 238 at ILL and 64 at ISIS. The ILL reactor resumed operation in September after a major shutdown for repairs and improvements which will keep it at the forefront of reactor-based neutron scattering research centres for the foreseeable future. The Laboratory continued its direct support of the Board's Neutron Beam Research Committee through the joint secretariat with SERC Central Office and also continued to support the irradiation programme carried out at the Herald reactor at AWRE, Aldermaston.

Experimental Science

Below are given brief descriptions of research projects in which members of the Laboratory have been engaged involving use of other facilities.

Dynamics of Proton Conducting Solids

The proton dynamics of 12-tungstophosphoric acid 14 hydrate have been investigated using incoherent quasi-elastic neutron scattering, in collaboration with Exeter University. Between 250 and 295 K, the observed motion is consistent with 180° jump reorientations of an H_2O molecule about its 2-fold axis with a correlation time of 10^{-10} s. The H_3O^+ reorientations are much faster than the H_2O reorientations whilst H^+ is too slow to be observed on the neutron time scale. These results are consistent with the interpretation of previous nuclear magnetic resonance data.

The H-atom transport mechanism in the oxide-insertion compound hydrogen molybdenum bronze, $H_{1.7}MoO_3$, has been studied using similar techniques. At 275 and 285 K, the H^+ translational diffusion is too slow to be observed and the $-OH_2$ groups are found to reorientate in a four-fold potential with an activation energy of $E_a \sim 24 \pm 0$ kJ mol^{-1} and $t_\infty \sim 10^{-15}$ s. On raising the temperature to 295 K, the motions of the $-OH_2$ groups can no longer be described in terms of a simple four-fold reorientation but now appear to be the combination of coupled rotational and translational diffusion processes.

Micellar Solutions

In collaboration with Oak Ridge National Laboratory and Unilever Research, work has continued on the structure of anisotropic micellar solutions aligned by viscous shear flow. Following the preliminary investigation of dilute cylindrical micelles of cetyltrimethyl ammonium bromide (CTAB), effort has concentrated on rod flexibility. Dodecyl dimethyl ammonium chloride (CCACl) is thought to produce more flexible rods than CTAB, and recently obtained data on DDACl will be evaluated in terms of flexibility.

The initial work on interacting systems focused on the viscoelastic phase of the mixed surfactant system, sodium dodecyl sulphate (SDS) and tetradecyl dimethyl ammonium propane sulphonate (TDPS). Data has been obtained on a further viscoelastic system CTAB/sodium parachlorobenzoate (SCB). Complete alignment was obtained at the remarkably low shear gradient of 50 s^{-1}. Analysis of the viscoelastic systems is in progress.

Covalence and Spin Polarisation in the $Cr(CN)_6^{3-}$ Ion

The hexacyano-complex ions of the transition series metals are commonly believed to involve some of the most covalent bonding to be found for those elements. The spin distribution, as it involves only the highest-lying orbitals, is particularly sensitive to bonding effects so a polarised neutron diffraction experiment has been carried out in collaboration with the Universities of Sussex and Western Australia on an extinction-free crystal of $Cs_2KCr(CN)_6$ at 4.2 K and in a magnetic field of 4.6 T using the D3 diffractometer at Institut Laue-Langevin. The magnetic structure factors were fitted using an atomic orbital model of $Cr(CN)_6^{3-}$ ion.

The model shows the spin to be concentrated in the t_{2g} orbitals with an 8% expansion in 3d radial dependence. There is a large diffuse metal-centred spin distribution ('4s + 4p') and a substantial (total 1.25 spins) ligand spin population. This large ligand contribution emphasises the strong metal-cyanide interaction. The σ density shows −0.47 spins on each cyanide group and 0.12 in the Cr e_g orbitals. The π density on the ligands shows negative spin on C and a large positive value on N. It seems that the high degree of covalence associated with the CN^- ion involves strong polarisation of the spin-paired bonding molecular orbitals, giving negative spin on the cyanide groups and positive on the chromium as expected qualitatively. This effect is at least as strong as the spin transfer from the Cr t_{2g} orbitals into the CN^- system by π-back-bonding.

X-ray Diffraction

A research programme to study the structures of liquid crystalline materials is under way using the MWPC X-ray diffraction facility. Progress has been made in fundamental studies of the smectic D liquid crystalline phase. This phase has been shown to possess primitive cubic symmetry, an unusually high degree of symmetry for this class of material. A typical X-ray diffraction pattern is shown in Fig 4.18. These data are being used to construct a micellar-type structural model for the smectic D phase. Studies have also been carried out with the aim of characterising in detail the technologically important smectic C phase in a range of liquid crystalline materials.

Crystal Monochromators

The idea of coupling the effects of coherent Bragg diffraction with the enhanced scattered length observed at a neutron absorption resonance to produce an

enhanced monochromatic Bragg reflection at electron-volt energies has been studied on a 2-circle diffractometer at the Harwell linac. Using a single crystal of UO_2, the (18,6,0) Bragg reflection was scanned through the energy of the ^{238}U 6.6eV resonance and an enhancement of the scattered intensity was observed when the energies of the Bragg reflection and the absorption resonance were coincident. The measurements showed that, in general, the effect of coherent resonant neutron diffraction is much weaker than the absorption so the method requires considerable development before a practical monochromator can be constructed.

Muon Spectroscopy and Chemistry

Muonium, the radioactive light isotope of hydrogen, may be used to label molecular radicals and provides a wealth of information on their physical and chemical properties. Isotope effects in particular are more pronounced than those obtained by deuteration or tritiation, the more common isotopic substitutions, and are more readily interpreted in terms of molecular structure, dynamics and electronic configuration.

Using μSR facilities available in Europe, support continued for the Leicester University Chemistry Department in this research, for which a second SERC grant and postdoctoral fellowship has been awarded this year. Following closure of the CJ2 muon beamline at CERN, experiments were pursued at SIN in collaboration with the University of Zürich. In studies of muonium addition at the carbonyl bond, new radicals were identified in the formate, acetate and formamide families. Here, the muon-electron hyperfine coupling is a particularly sensitive indication of the preferred radical conformation as well as the degree of delocalisation of the unpaired electron. New radicals were also identified in some cyclic compounds, offering the possibility of studying conformer interchange. The competition for muonium addition at the aromatic and olefinic bonds was studied in styrene and in allyl benzene.

A general study was undertaken of the systematics of muon-electron hyperfine coupling and the nature of the singly-occupied molecular orbital in muonated organic radicals. This emphasized the importance of conjugative effects in determining radical conformation, dynamical properties and muon-proton isotope effects. Molecular radical models were also found to account for the systematics of the hyperfine coupling in muonium centres in a variety of crystalline solids and provide the first satisfactory microscopic description of these centres.

Condensed Matter Theory

The range of topics on which research work is done has increased, largely through international collaborations. Visitors from Austria, China, Germany, Greece, Italy and the USA (some with financial support from the British Council and NATO) have participated in joint projects with RAL staff and consultants. New research work includes both timely studies and feasibility studies for new experiments with ISIS. A few topics which illustrate the diversity in the research programme are summarised in the following paragraphs.

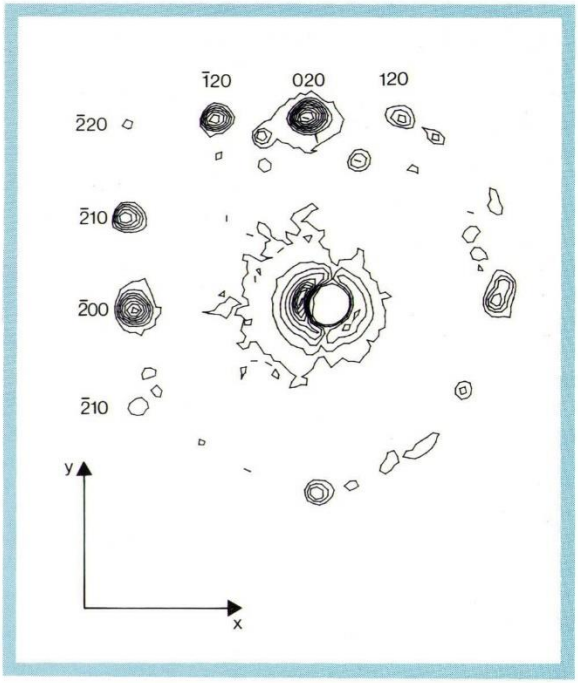

Fig 4.18 Contour map of a typical diffraction pattern of the smectic D phase of $C_{18}H_{37}O(C_6H_3)(CN)(C_6H_4)COOH$ at 175°C. Contours at the centre of the diffraction pattern represent scattering of the incident beam by the beam stop. The [020] reflections correspond to a scattering angle of ~2° (Cu KI radiation). The indexed peaks define two edges and a corner of a square, and this and similar data taken at different sample orientations show that the structure has cubic symmetry. Weaker reflections (not indexed) arise from other crystal domains within the sample.

Magnetic Colloids

Polystyrene spheres in a slab of strongly paramagnetic fluid crystallise when a magnetic field is applied normally. Long-range forces, associated with these dipole holes and their images, make the calculation of energies of the resultant structures very delicate. A new generalisation of the classic Ewald method for lattice sums has been developed. Square and triangular lattices are very close in energy. Displacements out of plane develop as instabilities according to density and slab thickness. Implications for switchable optical gratings, electronics and for models of two-dimensional (topological) melting are subjects of current work.

Neutron-Electron Spectroscopy of Rare Earths

Magnetic neutron-electron scattering induces transitions between spin-orbit split states of 4f electrons attached to rare earth ions. Because the separation of

most spin-orbit states exceeds 0.1eV, the spectroscopy demands epithermal neutrons, which are in copious supply from pulsed spallation neutron sources. Moreover, there is the possibility of avoiding strong nuclear absorption, characteristic of most heavy nuclei, by using a window between compound nuclear states. Calculations of the cross-section for transitions between the ground and excited states of tripositive rare earth ions reveal (a) dipole-allowed transitions at small scattering angles are much stronger than higher-order multipole transitions possible at intermediate angles and (b) the scattering angle dependence of the structure factors for dipole-allowed transitions are usually significantly different from elastic form factors.

Neutron-Electron Scattering from Band Electrons

Inelastic neutron scattering from conduction electrons in metals and semiconductors is an experimental method with potentially far reaching ramifications in materials science. The feasibility and usefulness of the method can be assessed by calculating the appropriate cross-section for realistic models of electrons in materials, using band structure theory, for example. Effects due to Coulomb, electron-phonon and magnetic field interactions are gauged from studies of exact sum rules for the cross-section, which can also serve as a guide to the validity of approximate, model calculations. Coulomb-induced electron correlations have been shown to be significant in the cross-section at intermediate wave vectors, and the long-wavelength response is changed dramatically by a magnetic field through the creation of Landau levels and coupling to the collective electron density oscillation.

Fig 4.19 Spherical liquid crystal droplet, with a sector removed to show the internal structure. The cylinders represent the orientation of the molecules and are tangential to the surface; lines are to guide the eye. Note the singularities at the poles.

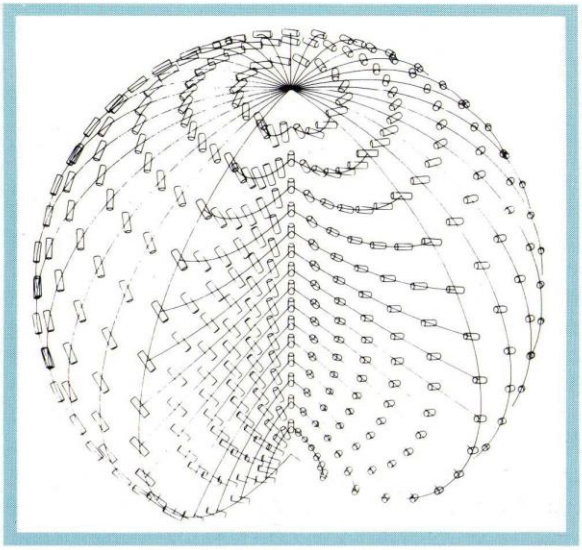

Granular Superconductors

In a regular array of Josephson junctions, as the size of the junctions is reduced below the 1μm scale, Josephson tunnelling has to compete with electrostatic influences in trying to set up a superconducting state. For sufficiently small junctions, the electrostatic influence dominates and a transition to an insulating state occurs. This has been studied, and the superconducting state can be considered to be Bose condensates of Cooper pairs and holes, unlike the bulk superconducting state. These condensates are coupled via an intrinsic Josephson Effect. It is predicted that experiments will determine that the excitation spectrum consists of two branches (the condensates oscillating in or out of phase with each other), the shape of which depends on the current carried.

Liquid Crystals

The rod-like molecules in nematic liquid crystals line up parallel to each other and molecule directors are correlated over macroscopic distances; furthermore, there is elastic energy associated with distortions of the director. At an interface between nematic and isotropic fluid, an important case is when the director is tangential to the interface. For a spherical droplet, part of a colloidal dispersion of nematic, there is a topological requirement for the director to have a point singularity on the surface of the sphere (the 'hairy ball' theorem) and the minimisation of elastic energy in the presence of the singularity gives rise to a twisted director field (Fig 4.19). If a magnetic field is present, the droplet will exhibit changes in twist, and reorientation if the field is strong enough. Polymers may be nematic (like uncooked rather than cooked spaghetti) and droplets of polymer nematic are predicted to be highly twisted. An obvious tool for investigation of these suspensions of droplets is the rotation of polarised light. With a non-tangential interface, the singularity structure is more complex, and lines of singularity appear in addition to the twisting and to the point singularities.